Interpretation of the Near-Infrared Absorption of Magnesium Phthalocyanine Complexes in Terms of Exciton Coupling Effects

A. Endo, S. Matsumoto, and J. Mizuguchi*

Department of Applied Physics, Faculty of Engineering, Yokohama National University, 79-5 Tokiwadai, Hodogaya-ku, 240-8501 Yokohama, Japan

Received: May 19, 1999

Magnesium phthalocyanine (MgPc) is a blue pigment whose X-phase is known to exhibit an intense near-IR-absorption. Because of this, MgPc has attracted attention as a material useful for laser printers as well as optical disks based on GaAsAl laser diodes. The near-IR absorption has, therefore, been investigated from the standpoints of exciton coupling effects on the basis of the crystal structure. Two kinds of six-coordinate MgPc complexes were grown from solution and their structures were analyzed: $MgPc/(H_2O)_2\cdot(N$-methyl-2-pyrrolidone$)_2$ (crystal **1**) and MgPc/(2-methoxyethanol)$_2$ (crystal **2**). In both crystals, two oxygen atoms of the solvent molecule are coordinated to the central Mg atom above and below the molecular plane, forming a distorted sp^3d^2 octahedron. Of these crystals, only crystal **1** exhibits a near-IR absorption whose spectral shape is quite similar to that of the X-phase. In addition, the X-phase is also found to contain two water molecules in the normal ambient atmosphere. The near-IR absorption in both crystal **1** and the X-phase can reasonably be interpreted as arising from exciton coupling effects based on the molecular arrangement of $MgPc/(H_2O)_2$.

1. Introduction

Magnesium phthalocyanine (MgPc) is known as a blue pigment that possesses several crystal modifications. Among these, only the X-phase exhibits an intense near-IR-absorption, as shown in Figure 1.[1−5] Because of this, MgPc has recently attracted attention as a material useful for laser printers[2,3] as well as for optical disks[4] based on GaAsAl laser diodes. The spectral shape of the near-IR absorption of MgPc is strikingly different from that of titanyl phthalocyanine (TiOPc), which is now widely used for laser printers in practice.[6−11] The former is characterized by a relatively narrow absorption band localized in the near-IR region (Figure 1), whereas TiOPc shows a very broad band from the visible to the near-IR region. The near-IR absorption of TiOPc has recently been interpreted in the framework of molecular distortion on going from solution to the solid state.[10,11] Heavy molecular deformation in phase II of TiOPc lifts the doubly degenerate excited state and causes an extremely large band splitting to occur, giving two absorption bands in the visible/near-IR region. The longer-wavelength component gives the near-IR absorption.

Since the elucidation of the near-IR absorption is basic to an understanding of the photoconduction mechanism, an attempt was made to characterize the near-IR absorption of MgPc from the standpoints of molecular distortion and exciton coupling effects (i.e., interactions between two transition dipoles) on the basis of single crystals. In the course of our investigation, we encountered two kinds of solvated single crystals of MgPc when recrystallized from solution: $MgPc/(H_2O)_2\cdot(N$-methyl-2-pyrrolidone$)_2$ (crystal **1**) and MgPc/(2-methoxyethanol)$_2$ (crystal **2**). Of these crystals, only crystal **1** is found to exhibit an intense near-IR absorption whose spectral shape is very similar to that of the X-phase shown in Figure 1.

The present paper deals with the mechanism of the near-IR absorption of crystal **1** and the X-phase in terms of molecular distortion as well as exciton coupling effects based on the molecular arrangement of the MgPc complexes.

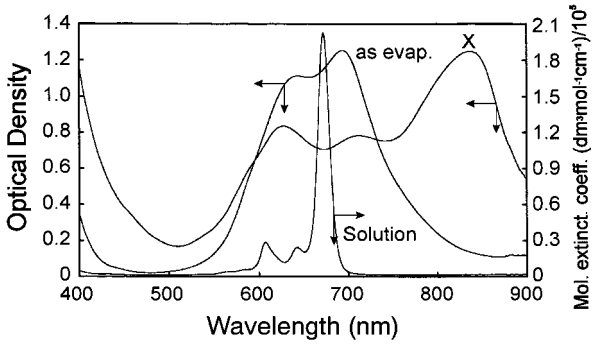

Figure 1. Solution spectrum as well as solid-state spectra of evaporated MgPc of "as evaporated" and the X-phase.

2. Experimental Section

2.1. Crystal Growth from Solution. MgPc was purchased from Tokyo Chemical Industry and purified three times by sublimation using a two-zone furnace.[12] The solvated single crystals were grown by recrystallization from *N*-methyl-2-pyrrolidone (NMP) and 2-methoxyethanol for complexes of $MgPc/(H_2O)_2\cdot(NMP)_2$ (crystal **1**) and MgPc/(2-methoxyethanol)$_2$ (crystal **2**), respectively. The dimensions of the single crystals were $0.2 \times 0.05 \times 0.5$ mm for crystal **1** and $0.1 \times 0.1 \times 0.3$ mm for crystal **2**. (The single crystals were also grown from the vapor phase but were found to rapidly polycrystallize in the normal ambient atmosphere, probably due to moisture in the air.)

2.2. Preparation of Evaporated Films. The evaporated thin film of MgPc was prepared using conventional vacuum evaporation equipment (Tokyo Vacuum Co. Ltd.: model EG240). The samples for measurements of visible absorption spectra were

10.1021/jp991624y CCC: $18.00
Published on Web 09/23/1999

TABLE 1: Crystallographic Data for Crystals 1 and 2

	crystal **1**	crystal **2**
formula	$MgPc/(H_2O)_2(NMP)_2$	$MgPc/(CH_3OCH_2CH_2OH)_2$
formula weight	773.15	689.03
crystal system	monoclinic	monoclinic
space group	$P2_1/n$	$P2_1/n$
Z	2	2
a (Å)	6.876(2)	12.37(1)
b (Å)	21.427(4)	8.078(6)
c (Å)	12.994(6)	17.974(9)
β (deg)	102.20(2)	109.70(7)
V (Å^3)	1871(1)	1690(2)
ρ_{calc} (g/cm^3)	1.375	1.354
ρ_{meas} (g/cm^3)	1.38	1.37

prepared onto plain glass slides, using the vacuum evaporation technique (film thickness: about 1000 Å). Evaporated layers of MgPc were exposed to acetone vapor for several hours to bring about the spectral change to give the X-phase.

2.3. Measurements. UV−vis spectra were recorded on a Shimadzu UV-2400PC spectrophotometer. Measurements for polarized reflection spectra were made on single crystals **1** and **2** by means of a UMSP 80 microscope-spectrophotometer (Carl Zeiss). An Epiplan Pol (×8) objective was used together with a Nicol-type polarizer. Reflectivities were corrected relative to the reflection standard of silicon carbide. Thermogravimetric analysis (TGA) was made for the X-phase of MgPc with a Rigaku Thermo Plus 8230. The sample was prepared by stripping the material from evaporated MgPc of the X phase.

2.4. Molecular Orbital (MO) Calculations. The geometry of the MgPc molecule was optimized by means of the INDO/1 Hamiltonian in the ZINDO program package.[13] The INDO/S program used for spectroscopic calculations is part of the ZINDO program package. Optical absorption bands for the solution were computed on the optimized geometry while the calculation for the molecule in crystals **1** and **2** was made on the basis of the X-ray *x*, *y*, *z* coordinate sets using the INDO/S Hamiltonian. A total of 197 configurations were considered for the configuration interaction (CI). All calculations were performed on a Power Macintosh 8500/120 computer.

3. Results and Discussion

3.1 Structure of Crystals 1 and 2.[14] *Molecular Conformation*. The crystallographic data are summarized in Table 1. Crystals **1** and **2** belong to the same crystal system (monoclinic) and the same space group ($P2_1/n$). In both crystals, two O atoms of the solvent molecules are coordinated to the central Mg atom, as shown in Figure 2, forming two kinds of deformed octahedron complexes: $MgPc/(H_2O)_2\cdot(NMP)_2$ and MgPc/(2-methoxyethanol)$_2$. The sp^3d^2 hybrid structure of the Mg atom accommodates six ligands, four of which are the surrounding nitrogen atoms on the molecular plane and two of which are the O atoms of the solvent molecules positioned above and below the molecular plane. Up to now, no six-coordinate MgPc complexes were known, although two sorts of five-coordinate MgPc have been reported: $[MgPc/(H_2O)\cdot(C_5H_5N)_2]$[15] and (PNP)[Mg(Cl)Pc]$CH_3COCH_3$,[16] where PNP denotes bis(triphenylphosphine)iminium.

Molecular Arrangement. Figure 3 shows the projection of the crystal structure onto the (*a*, *b*) plane (crystal **1**) and the (*b*, *c*) plane (crystal **2**). The molecules are stacked in a herringbone fashion along the *a*-axis and the *b*-axis for crystals **1** and **2**, respectively. In crystal **1**, two kinds of stacking columns are formed side by side: one is the column composed of MgPc/$(H_2O)_2$ and the other is based on NMP molecules. Since the interplanar spacing along the *a*-axis is relatively small (about 3.26 Å), the interaction between translationally equivalent molecules is expected to be relatively large. On the other hand, the interaction along the *b*-axis between two translationally inequivalent molecules is considered small because of the spacer of the NMP molecules between the MgPc/$(H_2O)_2$ columns. In crystal **2**, the situation is quite different. There is one kind of stacking column composed of MgPc/(2-methoxyethanol)$_2$ along the *b*-axis. The interplanar spacing is much larger than that of crystal **1** (about 7.40 Å), since there are two solvent molecules between MgPc molecules working as the spacer. This indicates that the interaction along the stacking axis in crystal **2** is appreciably smaller as compared with that of crystal **1**. On the other hand, the interaction between translationally inequivalent molecules in crystal **2** is significantly larger than that in crystal **1**, because the stacking columns are arranged directly side by side in crystal **2**.

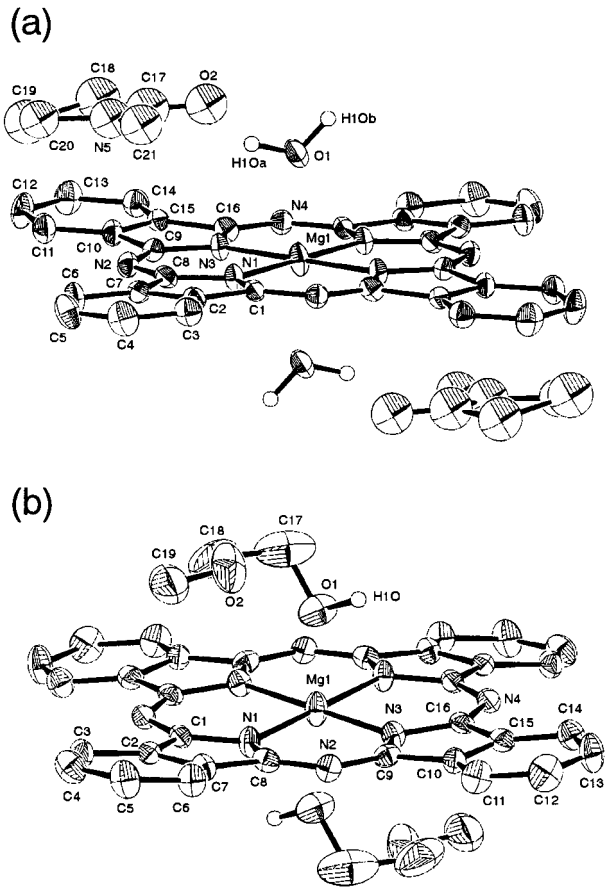

Figure 2. Molecular conformation of the solvated complexes: (a) $MgPc/(H_2O)_2(NMP)_2$ (crystal **1**) and (b) MgPc/(2-methoxyethanol)$_2$ (crystal **2**). H atoms except for those of the water molecule and the hydroxyl group are omitted for clarity.

3.2. Molecular Distortion and Its Effect on the Optical Absorption. Molecular distortion is known to lift the degeneracy of the excited state to give a profound influence on the optical absorption, particularly in TiOPc.[10] Therefore, the extent of molecular distortion was evaluated by measuring the angles between the plane of the four central nitrogen atoms (N1, N2, N3, and N4: plane 1) and the plane of each phenyl ring (plane 2) as shown in the inset of Table 2. If these angles are equal, this is taken as D_{4h} symmetry. The angles are listed in Table 2 together with those of the optimized geometry, which corresponds to the conformation in solution. It is apparent that the molecular symmetry for both crystals **1** and **2** is C_i, in contrast to D_{4h} assumed usually for MgPc in the free space. It is also recognized that crystal **2** is more distorted than crystal **1**.

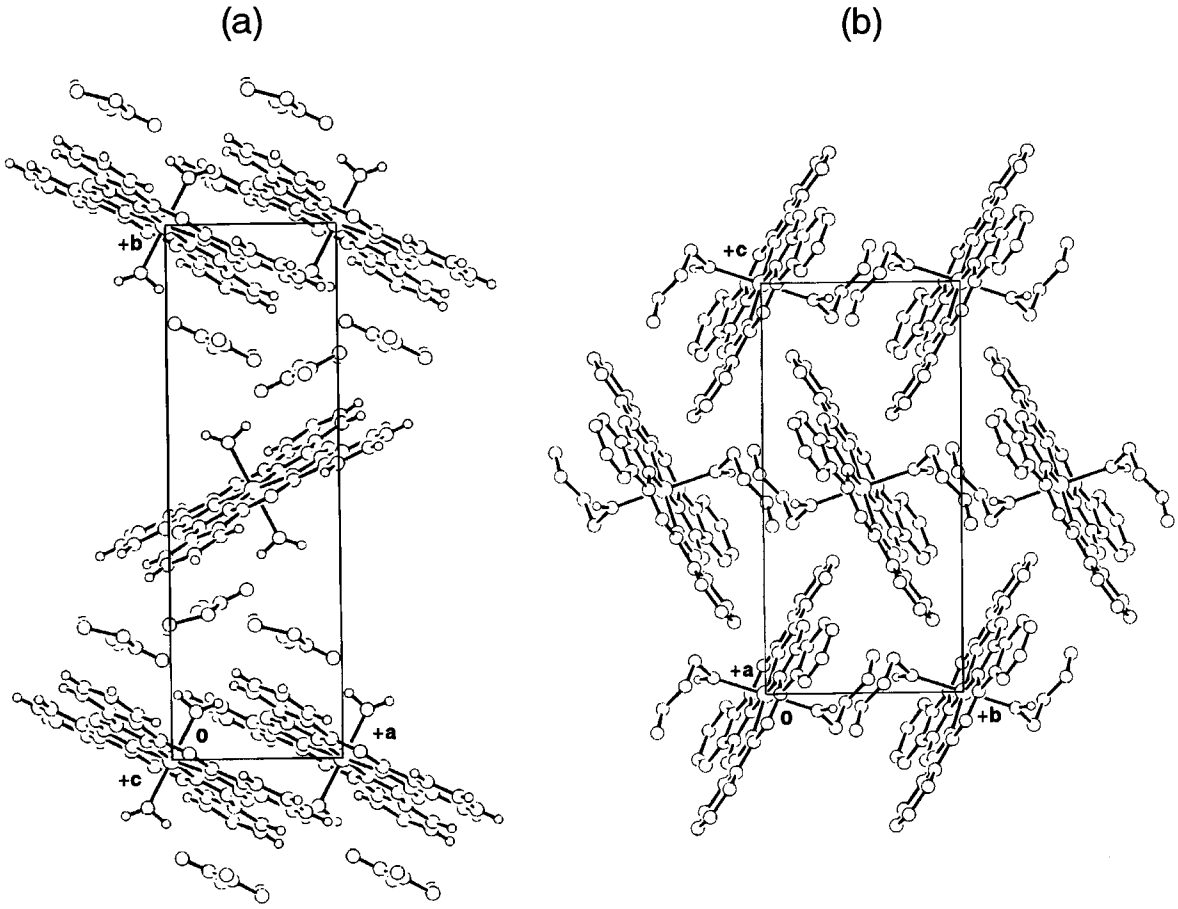

Figure 3. Projection of the crystal structure: (a) the (*a*,*b*) plane (crystal **1**) and (b) the (*b*,*c*) plane (crystal **2**).

TABLE 2: Molecular Distortion of the MgPc Skeleton in Crystals 1 and 2

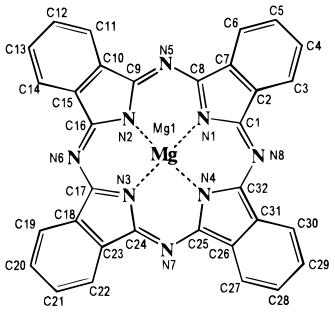

plane 1	plane 2	crystal **1**	crystal **2**	opt geo (solution)
N1,N2,N3,N4	phenyl C2···C7	−3.38°	−9.46°	0.0°
N1,N2,N3,N4	phenyl C10···C15	−1.46°	−13.51°	0.0°
N1,N2,N3,N4	phenyl C18···C23	+3.38°	+9.46°	0.0°
N1,N2,N3,N4	phenyl C26···C31	+1.46°	+13.51°	0.0°
symmetry		C_i	C_i	D_{4h}

The influence of the molecular distortion on the optical absorption was best evaluated by spectroscopic calculations using the X-ray *x*, *y*, *z* coordinate sets of crystals **1** and **2**. The calculated bands and their oscillator strengths are shown in Table 3 together with the direction of the transition moments A and B. The calculations were made for one single MgPc molecule as well as two kinds of solvated complexes in order to study the effect of the ligand on the optical absorption.

Since the excited state is doubly degenerate due to D_{4h} symmetry in the optimized geometry, $\pi-\pi^*$ transitions A and B give the identical absorption band. In fact, one single absorption band around 670 nm is observed in solution, as shown in Figure 1. The effect of molecular distortion of MgPc is clearly recognized in the form of the split bands A and B. As expected, the band splitting is larger in crystal **2** than in crystal **1**, because the former molecule is more distorted than the latter. Also recognized is the effect of the coordination ligand on the absorption band in MgPc/$(H_2O)_2$(NMP)$_2$ and MgPc/(2-methoxyethanol)$_2$. Slightly more distortion is again noticed in MgPc/$(H_2O)_2$(NMP)$_2$.

As described above, the present band splitting in crystals **1** and **2** is quite small (roughly one-tenth of the TiOPc: 1830 cm^{-1} in phase II[10]). This evidently indicates that the molecular distortion is not the major effect in MgPc to cause the near-IR absorption to appear. Another mechanism due to exciton coupling effects is explored below.

3.3. Polarized Reflection Spectra Measured on Single Crystals. Parts a and b of Figure 4 show the polarized reflection spectra measured on single crystals for crystals **1** and **2**, respectively. In crystal **1**, two prominent bands appear around 625 and 690 nm for polarization perpendicular to the *a*-axis. In addition, an intense reflection shoulder is also observed around 752 nm in the near-IR region. On the other hand, the shoulder in the near-IR region becomes an intense band around 765 nm for polarization parallel to the *a*-axis while the two intense bands in the visible region almost disappeared. The fact that the visible bands appear and disappear with polarized light suggests that these bands are assigned to the same electronic transition and are also different in nature from the near-IR absorption band around 765 nm.

The reflection spectra for crystal **2** (Figure 4b) exhibit no near-IR absorption. An intense band appears around 704 nm

TABLE 3: Calculated Absorption Bands for MgPc, MgPc/$(H_2O)_2(NMP)_2$, and MgPc/$(CH_3OCH_2CH_2OH)_2$

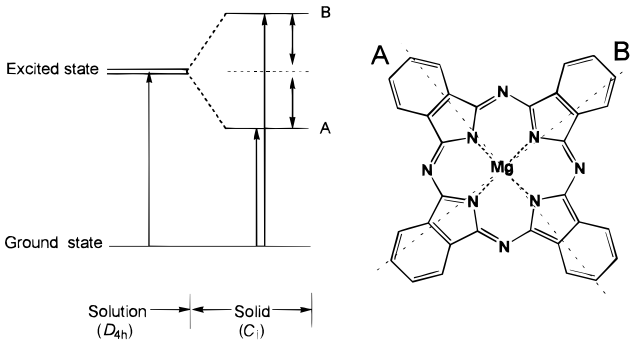

		opt geo		crystal **1**		crystal **2**	
		A	B	A	B	A	B
MgPc	λ_{max} (nm)	711.6	711.3	693.2	692.2	706.9	697.9
	f	0.9058	0.9068	0.9401	0.9029	0.9224	0.8736
		$\Delta\lambda = 0.3$ (7.0 cm^{-1})		$\Delta\lambda = 1.0$ (20.5 cm^{-1})		$\Delta\lambda = 9.0$ (183.5 cm^{-1})	
MgPc/$(H_2O)_2(NMP)_2$	λ_{max} (nm)			704.0	697.2		
	f			0.8821	0.8404		
				$\Delta\lambda = 6.8$ (137.9 cm^{-1})			
MgPc/$(CH_3OCH_2CH_2OH)_2$	λ_{max} (nm)					714.0	702.9
	f					0.8790	0.8235
						$\Delta\lambda = 11.1$ (221.9 cm^{-1})	

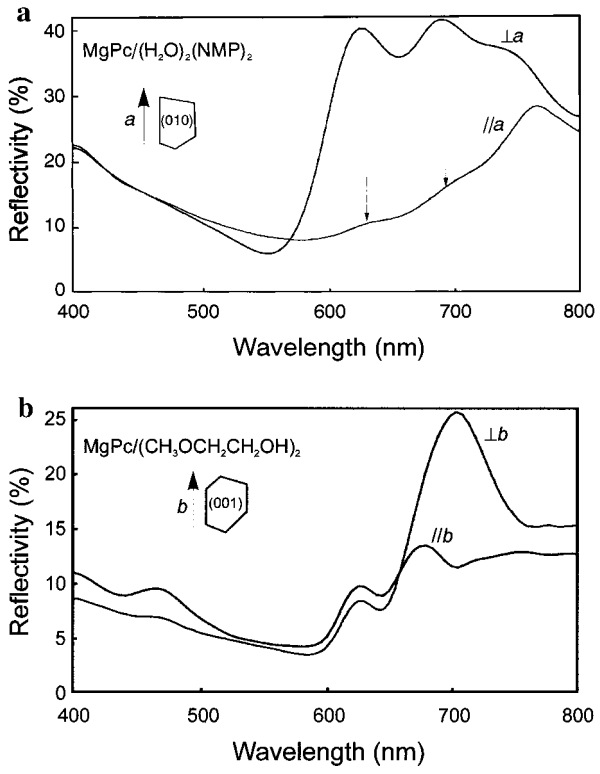

Figure 4. Polarized reflection spectra: (a) measured on the (010) plane for crystal **1** and (b) on the (001) plane for crystal **2**.

together with a small band around 625 nm for polarization perpendicular to the *b*-axis. Polarization parallel to the *b*-axis gives similar reflection bands around 625 and 667 nm, although the longer-wavelength band lies at a shorter wavelength by about 37 nm as compared with that for polarization perpendicular to the *b*-axis (704 nm). This difference is attributed to the Davydov splitting induced by two translationally inequivalent transition dipoles, as described below.

Judging from the above polarized reflection spectra, the two visible bands appear in common in both crystals while the near-IR absorption is additionally present only in crystal **1**. Furthermore, polarization parallel to the *a*-axis in crystal **1** greatly enhances the near-IR absorption but almost quenches the visible bands. These facts suggest that the near-IR absorption arises from exciton coupling effects; in other words, due to interactions caused by two translationally equivalent transition dipoles, as discussed in the next section.

3.4. Spectral Shifts or Davydov Splitting due to Exciton Coupling Effects. The molecular exciton coupling is defined by the excited state resonance interaction in loosely bound molecular systems.[17−20] As soon as the transition dipole appears on the molecule upon light excitation, the resonance interaction arises due to transition dipoles in translationally equivalent or inequivalent molecules to displace the excited energy level downward (red shift) or upward (blue shift) (depending on the relative orientation of the transition dipoles) or to induce the band splitting known as the Davydov splitting. The spectral shift will result between transition dipoles in translationally equivalent molecules ("parallel" or "head-to-tail" arrangement of the transition moments), whereas the Davydov splitting occurs due to an oblique arrangement of the transition dipoles in translationally inequivalent molecules. The present treatment has variously been employed in the interpretation of the absorption spectra in molecular crystals or dye aggregates: anthracene, perylene, naphthalene, and tetracene,[17−20] J-aggregates of cyanine dye stuffs,[21,22] dithioketopyrrolopyrrole pigment,[23] black perylene pigment,[24] and metal-free phthalocyanine.[25]

On the basis of exciton coupling model, the reflection spectra presented in the previous section can qualitatively be well interpreted by the molecular arrangement in crystals **1** and **2** (Figure 3a,b). As mentioned in section 3.1, the interaction between two translationally equivalent molecules along the stacking axis is larger in crystal **1** than in crystal **2.** On the contrary, the interaction between two translationally inequivalent molecules is larger in crystal **2** than in crystal **1**. This could

TABLE 4: Eight Neighboring Molecules around the Molecule at (000) and Their Displacement Energies

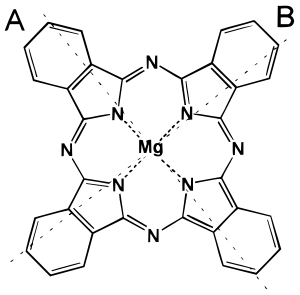

transition moment	site	no. of equiv molecules	r (Å)	θ (deg)	ΔE (cm^{-1})
		(a) Crystal **1**			
AA	(**1**,**0**,**0**)	2	6.860	50.80	−854
	(0,0,1)	2	13.000	54.85	2
	(1,0,1)	2	13.367	28.14	−770
	(1,0,−1)	2	15.920	78.48	300
BB	(**1**,**0**,**0**)	2	6.860	51.14	−686
	(0,0,1)	2	13.000	38.01	−478
	(1,0,1)	2	13.367	63.77	210
	(1,0,−1)	2	15.920	23.68	−456
total		16			−2730
		(b) Crystal **2**			
AA	(**0**,**1**,**0**)	2	8.078	65.52	1139
	(1,0,0)	2	12.370	84.86	640
	(1,1,0)	4	14.774	81.28	717
BB	(**0**,**1**,**0**)	2	8.078	65.52	2242
	(1,0,0)	2	12.370	168.37	−1335
	(1,1,0)	4	14.774	21.52	−1334
total		16			2070

suggest that the spectral shift plays the dominant role in crystal **1** rather than the Davydov splitting, while the Davydov splitting is the major effect in crystal **2** rather than the spectral shift. In fact, the near-IR absorption that corresponds to a large spectral shift toward longer wavelengths appears only in crystal **1** (Figure 4a); whereas the Davydov splitting is uniquely observed in crystal **2** (Figure 4b). An important question then arises whether the transition-dipole pairs that induce a large bathochromic shift exist in crystal **1** while no such pairs are present in crystal **2**. This will be answered in the next section.

3.5. Computations for the Exciton Displacement Energies in Crystals 1 and 2. The exciton displacement energy ($\Delta E_{\text{exciton}}$), which corresponds to the spectral shift is given by the following dipole−dipole equation:[17−20] $\Delta E_{\text{exciton}} = |\mu|^2(1 - 3\cos^2\theta)/r^3$, where the transition moment is denoted by μ and the distance and angle between two transition dipoles by r and θ, respectively. The term $(1 - 3\cos^2\theta)$ determines the geometrical relationship of transition dipoles correlated with the crystal structure. The bathochromic or hypsochromic shift depends on the critical angle of $\theta = 54.7°$, below which the former will result and above which the latter will be the case.

The exciton displacement energies are calculated for eight neighboring molecules for crystals **1** and **2**. The distance r and angle θ were obtained from the crystal structure for each crystal. The transition moments μ in crystals **1** and **2** were calculated on the basis of the X-ray x, y, z coordinate sets using the INDO/S Hamiltonian.[13] The transition moments A and B on the molecule are shown in the inset of Table 3. The results calculated for crystals **1** and **2** are set out in Table 4a,b, respectively. AA or BB denotes the coupling of transition moment A (or B) of one MgPc molecule with that (or B) of the neighboring one. The molecular sites are designated in fractional coordinates. The

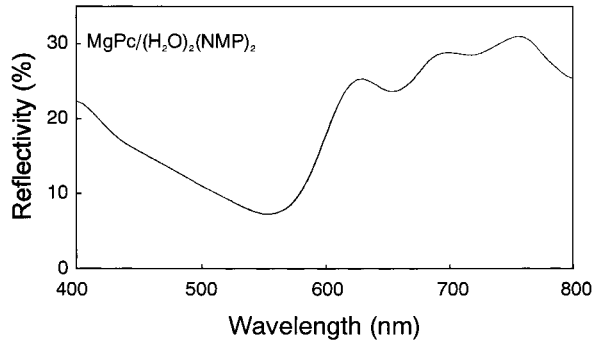

Figure 5. Averaged reflection spectrum of crystal **1** as obtained by superposition of the two polarized reflection spectra perpendicular and parallel to the *a*-axis (Figure 4a).

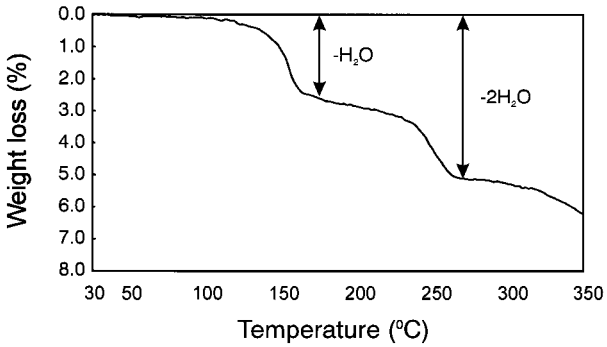

Figure 6. Weight loss of the powdered sample of the X-phase as a function of temperature.

minus or plus sign of ΔE denotes the bathochromic or hypsochromic displacement, respectively. In crystal **1**, five pairs are found to contribute to the bathochoromic shifts, leading to the displacement energy of about 2730 cm^{-1}. On the other hand, the calculation in crystal **2** results in the hypsochromic shift of about 2070 cm^{-1}. Judging from the direction of the spectral shifts for crystals **1** and **2**, it is evident that the near-IR absorption in crystal **1** arises from exciton coupling effects, although we need discussions for further details.

3.6. Near-IR Absorption in Crystal 1 and the X-Phase. Figure 5 shows the superposition of the two polarized reflection spectra for crystal **1** (Figure 4a). The present averaged spectrum is strikingly similar to that of the X-phase shown in Figure 1. It should also be remembered that the near-IR absorption in crystal **1** is due to exciton coupling effects based on the molecular arrangement of MgPc/$(H_2O)_2$(NMP)$_2$, in which MgPc/$(H_2O)_2$ and (NMP)$_2$ independently form their own stacking columns along the *a*-axis (Figure 3a). In addition, we are aware that the single crystal grown from the vapor phase rapidly polycrystallizes in the normal ambient atmosphere probably due to moisture from the air (section 2.1). These facts prompted us to assume that the X-phase includes water molecules in the form of MgPc/$(H_2O)_2$ while the sample is vapor-treated with acetone and that the near-IR absorption arises from exciton coupling effects based on the molecular arrangements of MgPc/$(H_2O)_2$. For this reason, we have carried out a thermogravimetric analysis (TGA) on evaporated films of the X-phase in order to justify the present assumption.

Figure 6 shows the weight loss of the powdered X-form as a function of temperature. The weight loss apparently occurs in two steps at about 160 and 260 °C and these correspond exactly to the weight loss of one molecule (H_2O/MgPc$(H_2O)_2$ = 3.14%) and two molecules (6.28%), respectively. This experiment evidently indicates that the X-phase is composed of MgPc/$(H_2O)_2$ and that the near-IR absorption is ascribed to

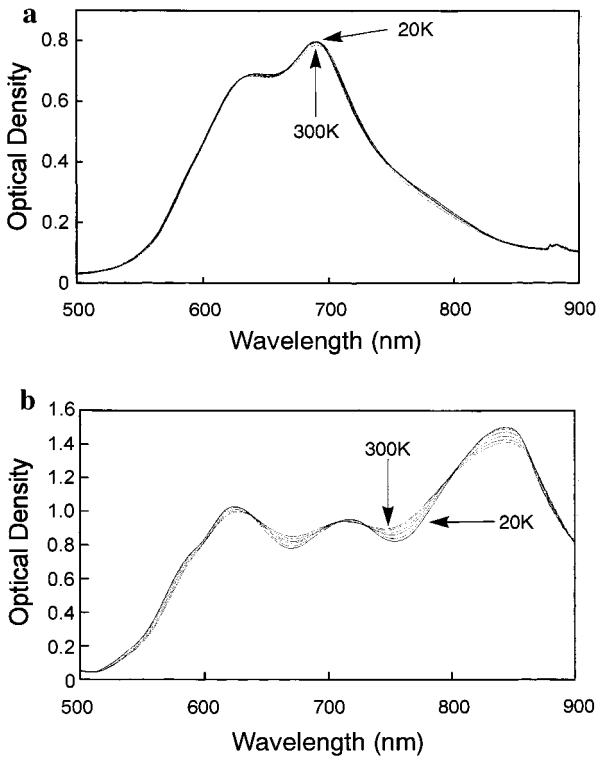

Figure 7. Temperature dependence of the absorption spectra of evaporated MgPc of "as evaporated" and the X-phase: (a) "as evaporated" (amorphous phase) and (b) X-phase.

the molecular arrangement of not MgPc but MgPc/$(H_2O)_2$. Furthermore, the X-ray diffraction analysis revealed that the interplanar spacing of the X-phase along the stacking axis (3.32 Å) is very close to that of crystal **1** (3.26 Å).

3.7. Temperature Dependence of the Absorption Spectra of Evaporated MgPc of "As Evaporated" and the X-Phase. Temperature dependence measurements of the absorption spectra are sometimes very useful in characterizing the electronic transition associated with molecular arrangement, because lattice contraction at low temperatures is expected to enhance intermolecular interactions, which, in turn, induce some change in absorption bands.

Parts a and b of Figure 7 show the temperature dependence of absorption spectra of evaporated MgPc of "as evaporated" (amorphous phase) and the X-phase, respectively, measured in the temperature range between 20 and 300 K. No significant temperature dependence is observed in the phase of "as evaporated". This is typical of isolated, randomly oriented molecules in the amorphous phase characterized by no significant intermolecular interactions. On the other hand, an appreciable temperature dependence is recognized, showing that each absorption band, particularly the near-IR band, is intensified upon lowering the temperature. This clearly indicates that the near-IR absorption band is very structure-sensitive and is due to intermolecular interactions. In other words, the absorption band is correlated with molecular arrangement.

3.8. Coordination of Two Water Molecules to MgPc. The tendency of accommodating water molecules into MgPc can first be attributed to the deliquescent properties of the magnesium atom. Magnesium is generally known to include water molecules upon crystallization to form six-coordinate complexes due to the sp^3d^2 hybridization: $MgCl_2 \cdot 6H_2O$,[26] $MgSO_4 \cdot 6H_2O$,[27] and $NH_4[Mg(H_2O)_6]Cl_3$.[28] This tendency is due to the relatively low basicity of Mg as compared with that of strontium and barium. The basicity, as characterized by electron-donating ability or low ionization potential, is the smallest in beryllium among the alkaline-earth metals and increases on descending the column in group IIA. In other words, beryllium, magnesium, and calcium are capable of accepting electron lone pairs of the oxygen atom of water or solvent molecules and are easily hydrated or solvated.[29] This explains why two O atoms of water or solvent molecules are coordinated to the Mg atom at the top and down apexes of the distorted sp^3d^2 octahedron.

Finally, we turn our attention to the mechanism of how the X-phase accommodates water molecules during the vapor treatment. Solvent vapor is known to induce molecular rearrangement to give a different phase. The phase change due to solvent vapor is considered to proceed in such a way that the vapor may loosen the crystal lattice, thus allowing the molecules to slide and/or rotate to find a more stable arrangement. In the presence of solvent vapor, we believe that the water molecule (contained in the solvent or moisture from the air) can easily be coordinated to MgPc. On the other hand, in the absence of solvent vapor, the crystal lattice is so rigid that the water molecules cannot diffuse sufficiently into the interstitial site of the crystal lattice. So the coordination of water occurs only near the surface. This notion is also supported by the fact that only incomplete phase change results when the evaporated film is directly immersed into water for several hours.

4. Conclusions

The near-IR absorption of the X-phase has been discussed on the basis of two kinds of solvated single crystals **1** and **2** from the standpoint of molecular distortion and exciton coupling effects. The conclusions drawn from the present investigation can be summarized as follows.

1. Two kinds of solvated single crystals have been obtained from solution: MgPc/$(H_2O)_2(NMP)_2$ (crystal **1**) and MgPc/(2-methoxyethanol)$_2$ (crystal **2**). In both crystals, the MgPc skeleton is found to be slightly deformed (C_i symmetry). The band splitting due to molecular distortion is, however, too small to cause the near-IR absorption to appear.

2. Crystal **1** exhibits an intense near-IR absorption around 765 nm, and this mechanism can be interpreted as arising from exciton coupling effects based on the molecular arrangement of MgPc/$(H_2O)_2(NMP)_2$.

3. The X-phase of MgPc is found to comprise MgPc/$(H_2O)_2$. The near-IR absorption can be explained in the same fashion as that of crystal **1**.

4. Coordination of water molecules to MgPc is ascribed to the inherent nature of the magnesium atom characterized by deliquescent properties.

References and Notes

(1) Hor, A. M.; Loutfy, R. O. *Thin Solid Films* **1983**, *106*, 291.
(2) Loutfy, R. O.; Hor, A. M.; DiPaola-Baranyi, G.; Hsiao, C. K. *J. Imag. Sci.* **1985**, *29*, 116.
(3) Khe, N. C.; Aizawa, M. *Nippon Kagaku Kaishi* **1986**, 393 (in Japanese).
(4) Daidoh, T.; Matsunaga, H.; Iwata, K. *Nippon Kagaku Kaishi* **1988**, 1090 (in Japanese).
(5) Kubota, H. G.; Muto, J.; Itoh, K. M. *J. Mater. Sci. Lett.* **1996**, *15*, 1475.
(6) Arishima, K.; Hiratsuka, H.; Tate, A.; Okada, T. *Appl. Phys. Lett.* **1982**, *40*, 279.
(7) Enokida, T.; Kurata, R.; Seta, T.; Katsura, H. *Denshi Shashin* **1988**, *27*, 533 (in Japanese).
(8) Fujimaki, Y.; Homma, T.; Moriguchi, H.; Watanabe, K.; Kinoshita, A.; Hirose, N.; Itani, A.; Ikeuchi, S. *J. Imag. Technol.* **1991**, *17*, 202.
(9) Saito, T.; Sisk, W.; Kobayashi, T.; Suzuki, S.; Iwayanagi, T. *J. Phys. Chem.* **1993**, *97*, 8026.
(10) Mizuguchi, J.; Rihs, G.; Karfunkel, H. R. *J. Phys. Chem.* **1995**, *99*, 16217.

(11) Mizuguchi, J.; Rihs, G. *Mol. Cryst. Liq. Cryst.* **1996**, *278*, 47.
(12) Mizuguchi, J. *Krist. Tech.* **1981**, *16*, 695.
(13) Zerner, M. C. *ZINDO, A General Semiempirical Program Package*; Department of Chemistry, University of Florida: Gainesville, FL.
(14) Matsumoto, S.; Endo, A.; Mizuguchi, J. *Z. Kristallogr.*, in press.
(15) Fischer, M. S.; Templeton, D. H.; Zalkin, A.; Calvin, M. *J. Am. Chem. Soc.* **1971**, *93*, 2622.
(16) Assmann, B.; Ostendrop, G.; Lehmann, G.; Homborg, H. *Z. Anorg. Allg. Chem.* **1996**, *622*, 1085.
(17) Kasha, M. *Spectroscopy of the Excited State*; Plenum Press: New York, 1976; p 337.
(18) Craig, D. P.; Walmsley, S. H. *Excitons in Molecular Crystals*; W. A. Benjamin, Inc.: New York, 1968.
(19) Hochstrasser, R. M.*Molecular Aspects of Symmetry*, W. A. Benjamin, Inc.: New York, Amsterdam, 1966.
(20) Davydov, A. S. *Theory of Molecular Excitons*; McGraw-Hill Book Co., Inc.: New York, 1962.
(21) Marchetti, A. P.; Salzberg, C. D.; Walker, E. I. P. *J. Chem. Phys.* **1976**, *64*, 4693.
(22) Norland, K.; Ames, A.; Taylor, T. *Photogr. Sci. Eng.* **1970**, *14*, 295.
(23) Mizuguchi, J. *Electrophotography* **1998**, *37*, 58.
(24) Mizuguchgi, J. *J. Appl. Phys.* **1998**, *84*, 4479.
(25) Mizuguchi, J.; Matsumoto, S. *J. Phys. Chem. A* **1999**, *103*, 614.
(26) Agron, P. A.; Busing, W. R. *Acta Crystallogr.* **1985**, *C41*, 8.
(27) Zalkin, A.; Ruben, H.; Templeton, D. H. *Acta Crystallogr.* **1965**, *17*, 235.
(28) Solans, X.; Font-Altaba, M.; Aguilo, M.; Solans, J.; Domenech, V. *Acta Crystallogr.* **1983**, *C39*, 1488.
(29) Duffy, J. A. *General Inorganic Chemistry*, 2nd ed.; Longmans, Green and Co. Ltd.: London, 1974.